

Bimodal analysis of sediment transport in mountain torrents using hydrophones and sediment traps

Hiroaki NAKAYA

Member, Grant Aid and Technical Cooperation Div. International Cooperation Bureau, MOFA

Measurement of sediment transport in mountain torrents is important to elucidate the nature of the process. Many obstacles have prevented long-term continuous measurement of natural river basins with a substantial scale, so only a few sporadic observations have been collected over short durations. Direct sampling, therefore, has recently been augmented by more indirect but stable methods (hereafter 'indirect methods') including a hydrophone pipe–microphone acoustic sediment-discharge measuring system (hereafter 'hydrophone system'). Hydrophone systems count the times (hereafter 'pulses') at which bedload sediments strike a steel pipe–microphone acoustic sensor. A statistical analytical method can be used to calibrate and estimate bedload amounts sampled by a sediment pit with a linear combination of pulses and flow discharges. Sediment discharges exhibit striking variability in orders of magnitude during flood events. However, researchers have not explicitly taken into account the volatile nature of sediment transport phenomena, as most quantitative studies have applied unitary analytical forms. In this study, three hydrophone systems were installed in 100- and 200-km²-scale river basins together with sediment trap pits. During floods, most sediment (approximately 80%) occurred within the first one-quarter of sediment sequences reordered in a descending manner. Therefore, sediment–hydraulic quantities were dissected into two sets: the upper quarter and the lower three-quarters. Frequency distributions of sediment–hydraulic quantities for each set were compared closely to differentiate the two sets based on a set of cutoffs using only direct methods. Bimodal analytical fitting forms were drawn for each set. The results revealed that at the time scale of flood events, the quantitative accuracy of sediment discharge estimates can be improved by dissecting sediment discharge phenomena into periods of concentrated and of minor occurrences, incorporating sediment discharge variation during the duration of floods.

Keywords: Bimodal analysis, hydrophone, indirect method, sediment discharge.

1. INTRODUCTION

Most studies about the sediment transport process in mountain streams have focused on developing theoretical and experimental bedload equations (Gomez et al., 1989; Gomez, 1991; Rickenmann, 1991; D'Agostino et al., 1999; Rickenmann, 2001; Yager et al., 2007; Ancey et al., 2008). Difficulties associated with field observation have been major obstacles to testing and applying these equations properly. Direct sediment sampling is often not possible; even when it is possible, it may not be effective due to its lack of durability. However, field measurements are indispensable to elucidate sediment discharge and transport phenomena in mountain torrents, as opposed to those observed in experimental flumes. Initially, field measurements were conducted using direct sampling, which provides data about sediment–hydraulic quantities such as flow discharge and trapped sediments (ASCE, 1975; Georgiev, 1990; Gomez, 1991; Lenzi, 2004). Direct sampling methods must overcome multiple obstacles to be conducted in a stable and

reliable way. Recently, more indirect but stable methods have been devised to incorporate broader physical variables and to alleviate the observational constraints inherent in direct sampling methods (Habersack et al., 2001, 2002; Bunte et al., 2004; Hoshino et al., 2004; Imaizumi et al., 2005; Rickenmann et al., 2007, 2008; Nakaya et al., 2007; Nakaya, 2008a, 2008b, 2009a, 2009b).

Physical variables related to sediment discharge and transport phenomena (hereafter 'the phenomena') can be described as primary or secondary, depending on how close the variables are to the phenomena. When river channel and sediment supply conditions are equal, sediment discharge phenomena at a river section can generally be described by flow discharge during major large-scale floods; these create an equilibrium sediment transport condition in which entire river cross-sections are fluidized (Gomez, 1989). Apart from flow discharge (hereafter 'FD'), a primary variable, many secondary factors have non-negligible influential effects on the phenomena under non-equilibrium conditions engendered by more frequent minor floods (Kleinhaus et al., 2002;

Lopes et al., 2007). Therefore, secondary sediment–hydraulic quantities (hereafter ‘sediment-related quantities’), such as the hydrophone pulses described in this paper, can reflect the intensity and variability of sediment transport phenomena better than can primary variables, and they should be incorporated based on observational examination of their properties (for more details see Nakaya, 2009a). Indirect methods can be used to obtain and incorporate relevant sediment-related quantities.

This study focused on bedload sediment discharge (hereafter ‘SD’), which plays a critical role in flooding and channel formation in mountain torrents. SD measurements were collected using a hydrophone system (Nakaya, 2008b). Hydrophone systems detect the phenomena by measuring sediment-related pulses caused by bedload sediments striking a steel pipe–microphone acoustic sensor installed in the river bed. Collision sounds gathered by a condenser microphone pass through a band-pass filter and are then electrically amplified by a specified factor and converted to square waves through waveshaping (the specified factor is called a ‘channel’ and has a designated number such as 16; this would be specified as ch16). A square waveform is counted as a pulse when its electric voltage exceeds 0.1 V.

SD records reveal a salient variation on a seasonal as well as a flood-event basis (Torizzo et al., 2003; Lenzi, et al., 2004; Nakaya et al., 2007; Nakaya, 2008a). Previous observational studies have revealed a three-digit variation in SDs, a one-digit variation in FDs, and a three-digit variation in pulses from hydrophone systems. The correspondence of variation ranges between SDs and pulses may provide a statistical rationale for the introduction of sediment-related quantity into SD analyses (Nakaya, 2008b).

In this study, SDs were directly measured using a sampling method of sediment trap pits. Sequential SD values were used to calibrate coefficients of analytical forms, developed for estimation by applying the indirect method. Calibration of SDs solely by FDs produces an index of sediment density from a proportional relationship between total bedload sediment volume and total flow water volume. Calibration solely by a sediment-related quantity produces an index of sediment volume per unit quantity, e.g., sediment volume per pulse, in the case of hydrophone systems. Analytical forms of a single factor can always yield total volume unbiasedness (hereafter ‘VUB’) of unity with observation cases used for calibration, which is defined as total bedload volume estimated by an

analytical form over volume observed by sediment trap pits. The nearer the VUB is to unity, better the analytical estimation is. However, observation revealed no straightforward proportional relationships among FDs, sediment-related quantities, and SDs. The SD values obtained by direct sampling of sediment trap pits were calibrated and regressed using various combinations of sediment-related quantities, resulting in a corresponding analytical form. Analytical forms can be categorized according to the number of independent variable(s) or factor(s) they use. Regressions were conducted without intercepts because SDs cannot flow without accompanying FDs or pulses. This study applied linear additive forms to ensure clarity of statistical examination. Estimated SD values obtained from single-factor analytical forms (hereafter ‘SF forms’) are statistically valid only for total aggregated amounts and are inadequate when applied to SDs measured by comparative tracking because this results in low sequential consistency (hereafter ‘SC’). Appropriate estimation requires statistical goodness of fit in terms of VUB and also of SC, to a degree. Previous research has tested combinations of FDs and sediment-related quantities to improve goodness of fit, where the former factor is a necessary condition and the latter is a sufficient condition with regard to sediment discharge and transport phenomena (Nakaya, 2008b). A linear additive analytical form (hereafter ‘LA form’) of FDs and pulses has exhibited promising statistical goodness of fit both for short-term event-based flood case studies and for long-term yearly-based comparative studies with reservoir sedimentation (Nakaya, 2008a).

Coefficients of the linear additive form represent sediment volume per pulse and sediment density, respectively, so these can be used for comparison with other observational and analytical studies and for in-depth exploration of physical processes, when applied with due caution to their interaction.

Case studies have revealed that the quantitative accuracy of SD estimators can be improved by introducing a two-variable LA form (Nakaya, 2008a). To date, measured SDs and sediment-related quantities have been analyzed unitarily without explicitly considering variation in SDs during floods (Nakaya, 2008a, 2008b). However, observations have shown that SD phenomena occur not in a unitary manner but rather in a discrete and concentrated manner within sporadic and limited durations (Warburton, 1992; Rickenmann, 2001, 2007; Habersack et al., 2001 and 2002; Lenzi et al., 2004). Therefore, this study investigated SD

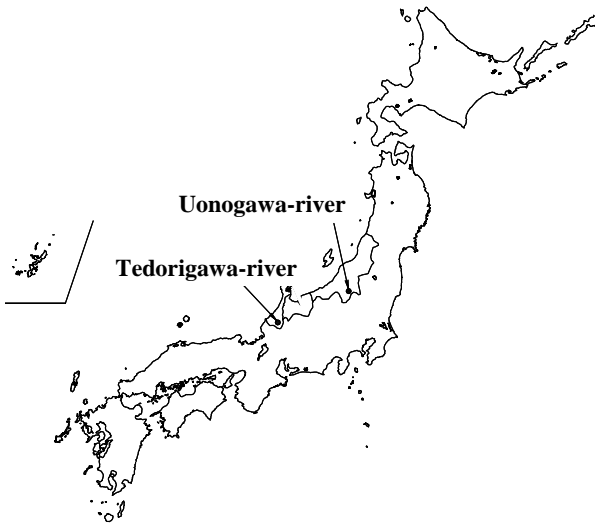


Fig.1 Locations of observation sites and rivers in Japan
 1) Uonogawa-river (Yuzawa Sabo Office, MLIT): 2 sites at the right and central section, downstream of the Onoharabashi bridge
 2) Tedorigawa-river (Kanazawa Office, MLIT), 1 site at the central section of Seto Sabo dam

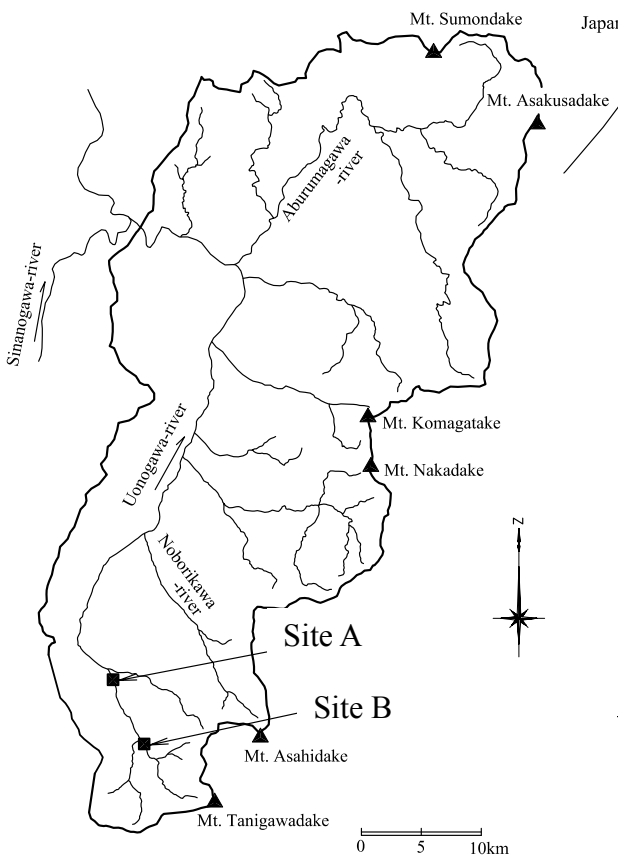


Fig.2 Location of observation site (Onoharabashi, Uonogawa-river)
 Site A: Onoharabashi site ($A = 97.6 \text{ km}^2$)
 Site B: Upperstream Tsuchitaru Sabo-dam ($A = 33 \text{ km}^2$)

phenomena in terms of their discrete and concentrated nature based on field observations, the characteristics of which are incorporated in the

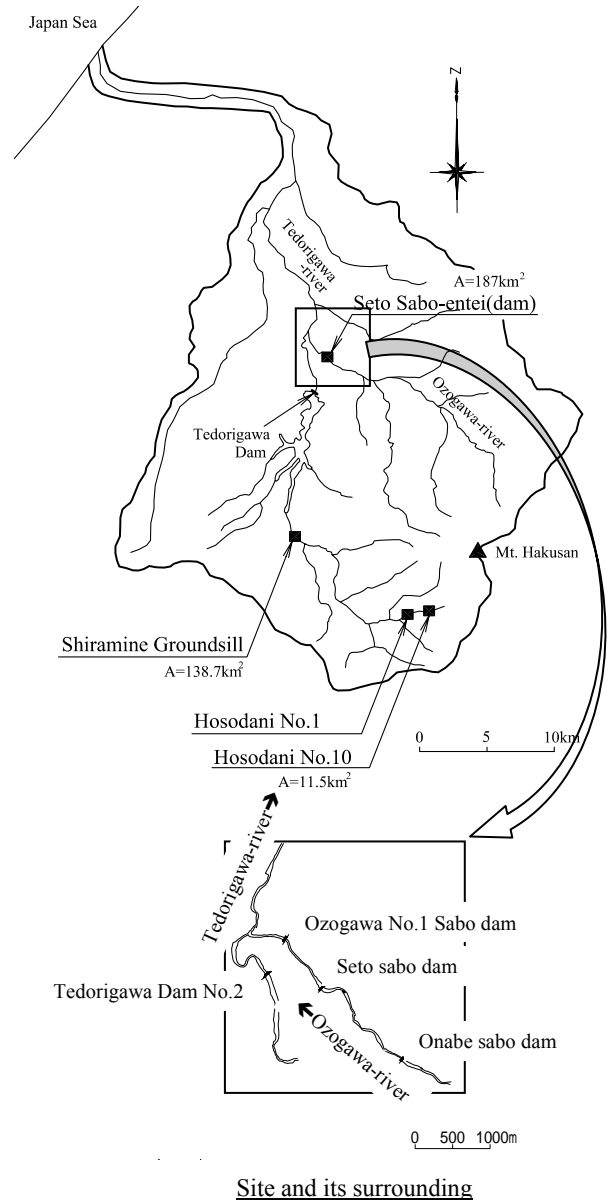


Fig.3 Location of observation site: Seto sabo dam, Ozogawa-river

bimodal quantitative analytical estimation method.

2. OBSERVATION SITES, MEASURING METHOD, AND OBSERVATION RESULT

Simultaneous SD observations were conducted using direct sampling by hydrophone systems at 10-minute intervals at three observation sites in the Hokuriku region. Figure 1 shows the locations of observation sites and rivers in Japan, and Figs. 2 and 3 show observation sites in a tributary of the Shinanogawa River and of the Tedorigawa River respectively (hereafter, the two sites on the Uonogawa River are sometimes referred to as 'Onoharabashi sites' and the site on the Ozogawa River is referred to as the 'Seto site').

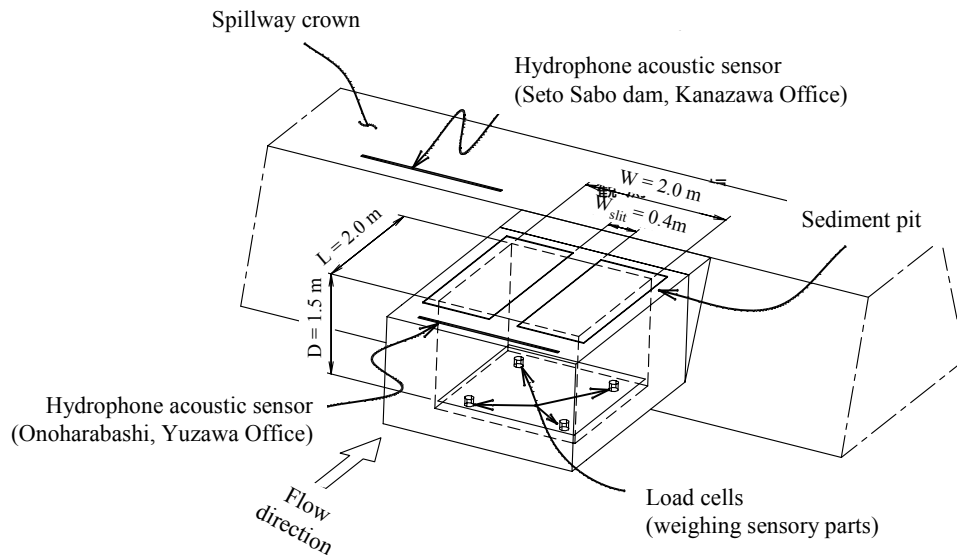


Fig. 4 Arrangement of sediment pit trap and hydrophone acoustic sensor

Table 1 Overview of observation sites

Observation sites	Onoharabashi site, Seto site, Unonogawa-river	Ozogawa-river
Catchment size of tributary basin	1504 km ²	189.52 km ²
Catchment size upstream of the site	97.6 km ²	186.98 km ²
River bed gradient	1/42	1/325
Average river width	40 m	45 m
Bed material d ₅₀	49.1 mm	14.7 mm
Roughness of river bed	0.045 s/m ^{1/3}	0.05 s/m ^{1/3}

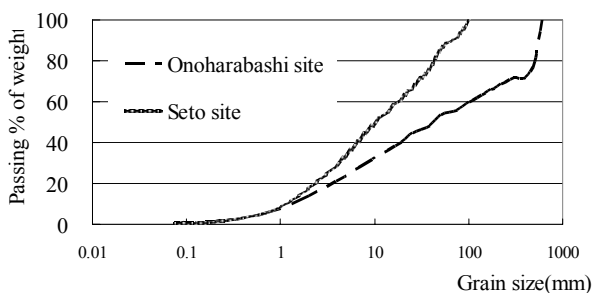


Fig.5 Grain size distributions for each observation site

Table 1 proves an overview of the observation sites. Figure 4 illustrates the arrangement of a sediment trap pit and hydrophone acoustic sensor. A sediment trap pit with load cells (weight sensors) measured the incremental load of incoming bedload sediment and converted the recorded loads into sediment volume using grain-size information obtained from pit sampling. In this study, bedload sediment flowing down over the slit width was considered to be entirely trapped by the pit. Figure 5

depicts grain-size distributions of river bed materials for each observation site (for a more detailed description of sediment trap pits for direct sampling and hydrophone systems, see Nakaya, 2007, 2008b).

Relationships among hydraulic quantities such as water stages and flow discharges were assessed from flow measurements at the Onoharabashi site and the Seto site. Relationships between water stage H (m) and total cross-sectional flow discharge Q (m³/sec), as well as those between the ratio of Q over unit width flow discharge q (m³/sec/m) and Q were first constructed analytically and then approximated by low-order power forms of Equations (1) and (2) (hereafter, Q is referred to as ‘total flow discharge’ or ‘total FD’). Here, the relationship between water stage H and total flow discharge Q is expressed to the second order, and that of the flow discharge ratio to the fourth order (coefficients, scope of application, and coefficients of determination of the forms at each observation site are described in detail in Nakaya, 2008b).

$$Q = \alpha_0(H + \alpha_1)^2 \tag{1}$$

$$\frac{Q}{q} = \beta_0 + \beta_1 Q + \beta_2 Q^2 + \beta_3 Q^3 + \beta_4 Q^4 \tag{2}$$

In total, 44 observation cases were analyzed: 16 cases from the right section of the Onoharabashi site, 13 from the central section of the Onoharabashi site, and 15 cases from the central section of the Seto site. Of the cases at the Onoharabashi site, 12 were analyzed simultaneously at the right and central section. The cumulative observation duration (site-time) for all sites was 1352 hours 15 minutes net, after subtracting null or unobserved durations. Table 2 provides an overview of the observation cases at each site. Here, pulses are represented using

Table 2 Overview of observation cases

Observation site	No. of observation case	Observation period	Flood duration time(hr)	Total flow discharge		Total sediment discharge*		Unit width pulse(P_{16})	
				Peak flow discharge (m^3/sec)	Total flow volume(m^3)	Peak discharge (m^3/sec)	Total load(m^3)	Max (/m/sec)	Sum(m)
Right section of Onoharabashi site, Unonogawa-river	OR1	2004/9/29-30	17:20	6.07×10	1.67×10^6	1.14×10^{-1}	3.83×10^2	6.87	9.64×10^4
	OR2	2005/4/7-5/9	791:25**	3.68×10	1.87×10^7	3.05×10^{-3}	2.88×10^2	3.68	2.24×10^4
	OR3	2005/6/28-29	47:30	3.76×10	1.05×10^6	4.82×10^{-3}	3.09×10	5.45	1.13×10^5
	OR4	2005/7/26-27	46:00**	5.82×10	2.28×10^6	4.90×10^{-2}	2.87×10^2	7.51	1.45×10^5
Central section of Onoharabashi site, Unonogawa-river	OC1	2006/10/6	8:10	3.00×10	7.11×10^5	1.49×10^{-2}	1.58×10^2	5.74	9.64×10^4
	OD1	2008/3/24	13:35	3.00×10	5.83×10^5	2.78×10^{-2}	1.49×10	4.59	2.24×10^4
	OD2	2008/4/7-10	60:20	2.03×10	3.24×10^6	7.62×10^{-2}	6.87×10	4.57	1.13×10^5
	OD3	2008/4/10-13	61:55	2.30×10	4.20×10^6	1.15×10^{-2}	5.65×10	4.31	1.45×10^5
	OD4	2008/4/17-25	193:55	4.47×10	1.73×10^7	7.78×10^{-2}	1.16×10^2	9.32	6.10×10^5
	OD5	2008/5/20	20:50	6.96×10	2.40×10^6	4.17×10^{-2}	1.59×10	1.05×10	2.20×10^5
	OD6	2008/6/23	12:40	1.27×10^2	1.28×10^6	3.32×10^{-2}	6.84×10	1.08×10	1.72×10^5
	OD7	2008/6/29	8:00	2.14×10	4.69×10^5	1.55×10^{-2}	2.69	4.75	3.85×10^4
	OD8	2008/7/7	9:10	2.38×10	5.13×10^5	1.55×10^{-2}	4.28	3.98	3.24×10^4
	OD9	2008/7/27	5:10	3.66×10	4.60×10^5	1.03×10^{-2}	6.84	9.57	6.29×10^4
	OD10	2008/8/5-6	15:40	5.00×10	8.65×10^5	2.37×10^{-2}	3.18×10	1.06×10	9.93×10^4
	OD11	2008/8/19	7:25	3.85×10	8.51×10^5	3.80×10^{-3}	1.84×10	7.23	4.66×10^4
OD12	2008/9/22	4:20	4.26×10	4.77×10^5	7.65×10^{-3}	1.43×10	7.09	2.10×10^4	
Right and central sections of Onoharabashi site (simultaneous observation)	SC1	2004/12/5	15:50	1.36×10	5.80×10^5	3.41×10^{-2}	1.89×10^2	2.16	4.73×10^4
	SC2	2005/6/28	2:25	1.22×10^2	6.62×10^5	1.53×10^{-1}	2.45×10^2	4.50	1.51×10^4
	SC3	2006/11/11	11:50	1.30×10	3.52×10^5	2.58×10^{-2}	2.07×10^2	2.48	2.30×10^4
	SC4	2007/2/14	3:20	2.70×10	2.01×10^5	6.07×10^{-2}	2.75×10^2	2.29	1.83×10^4
	SC5	2008/3/14-15	17:40	2.70×10	6.16×10^5	4.00×10^{-3}	1.98×10	2.58	1.93×10^4
	SC6	2008/4/10-11	34:30	7.22×10	5.57×10^6	2.44×10^{-3}	5.67×10	3.81	1.40×10^5
	SC7	2008/4/18	23:50	6.73×10	4.10×10^6	1.91×10^{-3}	2.54×10	3.56	4.30×10^4
	SC8	2008/4/24-25	27:50	7.74×10	4.96×10^6	2.16×10^{-3}	3.02×10	2.78	1.63×10^4
	SC9	2008/5/5-6	15:10	7.82×10	2.95×10^6	2.88×10^{-3}	1.66×10	4.39	5.55×10^4
	SC10	2008/5/20	14:00	3.68×10	1.02×10^6	4.71×10^{-3}	2.56×10	3.13×10^{-1}	1.64×10^3
	SC11	2008/5/25	16:50	1.02×10^2	3.18×10^6	8.40×10^{-3}	6.33×10	4.99	4.54×10^4
	SC12	2008/6/29-30	35:30	2.79×10^2	1.43×10^7	7.56×10^{-2}	1.40×10^2	5.23	1.39×10^5
	SC13	2008/8/19	2:50	9.92×10	5.90×10^5	8.90×10^{-3}	2.55×10	3.90	1.25×10^4
	SC14	2008/8/21	12:40	1.41×10	3.83×10^5	5.74×10^{-3}	3.79×10	2.95×10^{-1}	2.40×10^3
	SC15	2008/8/28-29	9:40	8.23×10	1.59×10^6	1.09×10^{-1}	2.04×10^2	3.47	2.97×10^4

*Converted to total sediment load by way of Q/q ratio. Data from the central section are shown for Onoharabashi site.

**Including void and unobserved periods, for individual cases

amplification level 16 (P_{16}), which yields adequate statistical correlation with SDs at the observation sites (Nakaya, 2007, 2008b). Total cross-sectional SDs Q_B were approximately derived by multiplying the ratio Q/q by unit width SDs obtained by sediment trap pits (hereafter, Q_B is referred to as 'total sediment discharge' or 'total SD'). This method of SD conversion (unit width into total width SDs) was applied throughout the study (for a more detailed discussion, see Nakaya, 2008a). The maximal peak FD of $Q = 2.79 \times 10^2$ (m^3/sec) was observed in case SC12 at the Seto site, and the maximal peak SD of

$Q_B = 1.53 \times 10^{-1}$ (m^3/sec) in SC2 at the Seto site. Total volumes of FD and SD, which are dependent upon flood durations, ranged from 2.01×10^5 to 1.87×10^7 (m^3) and 2.69 to 3.83×10^2 (m^3), respectively. Figure 6 shows the relationship between total FD and total SD using SC15 as an example. With the considerable variation in values, SDs behave in a different manner from FD.

When SD values reached their maximum for each case, unit width FDs and SDs were compared with theoretical sediment loads calculated by equilibrium bedload sediment formulas based on

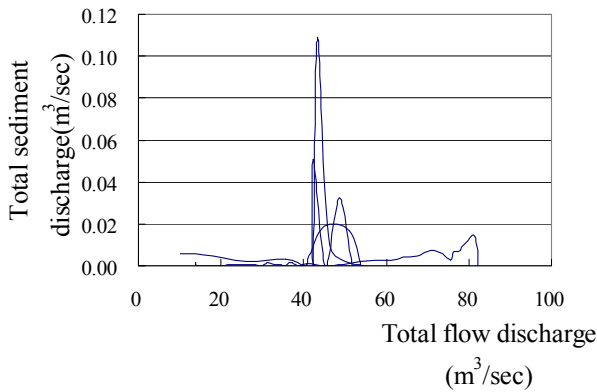


Fig.6 Relationship between flow and sediment discharge in observation case SC15 (at Seto site)

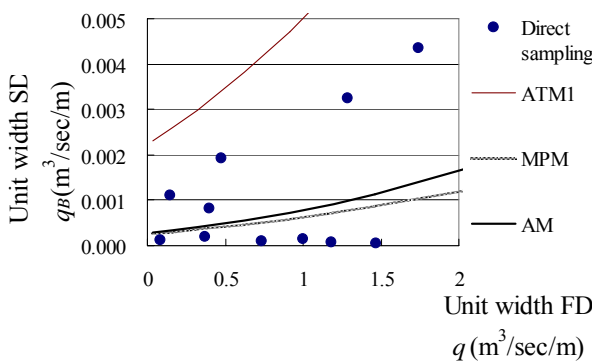


Fig.7 Relationship between observed unit width flow /bedload discharge and equilibrium bedload equations at the central section of Seto site when q_B is maximal in each case

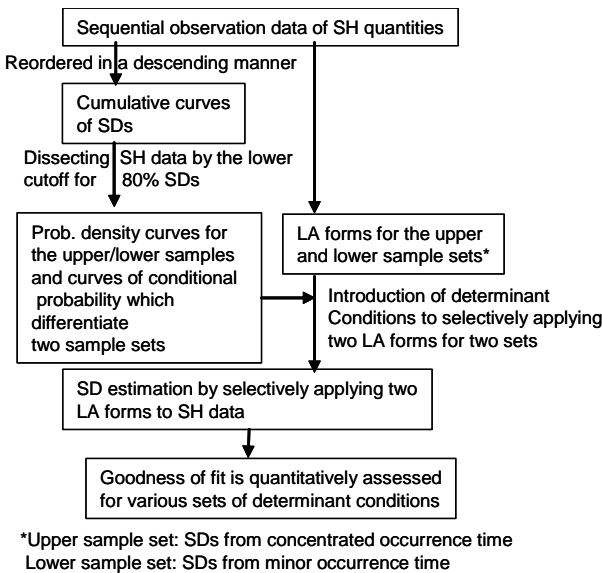


Fig.8 Outline of analytical method

FDs. The following formulas were applied: the Ashida–Takahashi–Mizuyama formula for steep channels (hereafter ‘ATM1’ to distinguish it from the formula used for less steep channels), the Meyer–Peter–Müller formula (hereafter ‘MPM’), and the Ashida–Michiue formula (hereafter ‘AM’)

(ASCE, 1975; Ashida et al., 1978, 1983; JSCE, 1999). A modified Egiazaroff formula was applied to calculate sediment loads of each grain size class, which were then summed to obtain sediment loads of all grain sizes, reflecting grain-size mixture effects. For ATM1, the modified Egiazaroff formula is not necessary, as it incorporates the effects in its derivation, using mean grain sizes. Figure 7 compares sediment loads based on measured and formula-based results for the Seto site, where some observed maxima were beyond MPM and AM, but all were below ATM1. Generally, observation cases were regarded as minor floods and not major large-scale flood events in which entire river cross-sections are fluidized, given the range of maximal SD points for all cases.

FDs, SDs, and pulses were all treated on a similar scale for unit time (per second) and unit width (per one meter in each channel cross section) to ensure coherence and consistency. Simultaneous observation cases from the right and central sections of the Onoharabashi site were assessed independently due to a large cross-sectional and sequential variation in sediment discharge. The catchment size ratio of Onoharabashi and Seto sites was approximately 1 to 2, the same as the ratio of river widths. This coincidence enabled observations of Onoharabashi and Seto sites to be treated as statistically homogeneous; the values fell within a similar range upon conversion to the unit width scale. All observation cases, therefore, were integrated in this study as one universal set of samples for analysis and examination. The same methodology was applied to observation cases for each site independently and yielded similar results (results are not shown due to space constraints).

3. ANALYTICAL METHODOLOGY

Analyses were based on basic sediment–hydraulic (hereafter ‘SH’) observation data: time series of SD q_B obtained by direct sampling, FD q , and pulse p_{16} expressed in unit time and unit width (hereafter, lowercase q_B , q , and p_{16} refer to unit time and unit width; descriptors of unit time and unit width are omitted whenever misunderstanding is unlikely). Basic SH observation data were analyzed to quantify the extent to which SD phenomena were discrete and concentrated in their time series. Intensities of pulses and FDs in the set of aggregated discrete and concentrated periods were compared with those in the other remnant set (hereafter referred to as ‘concentrated’ and ‘minor’ occurrence times, respectively). Determinant conditions by pulses and FDs were investigated in an

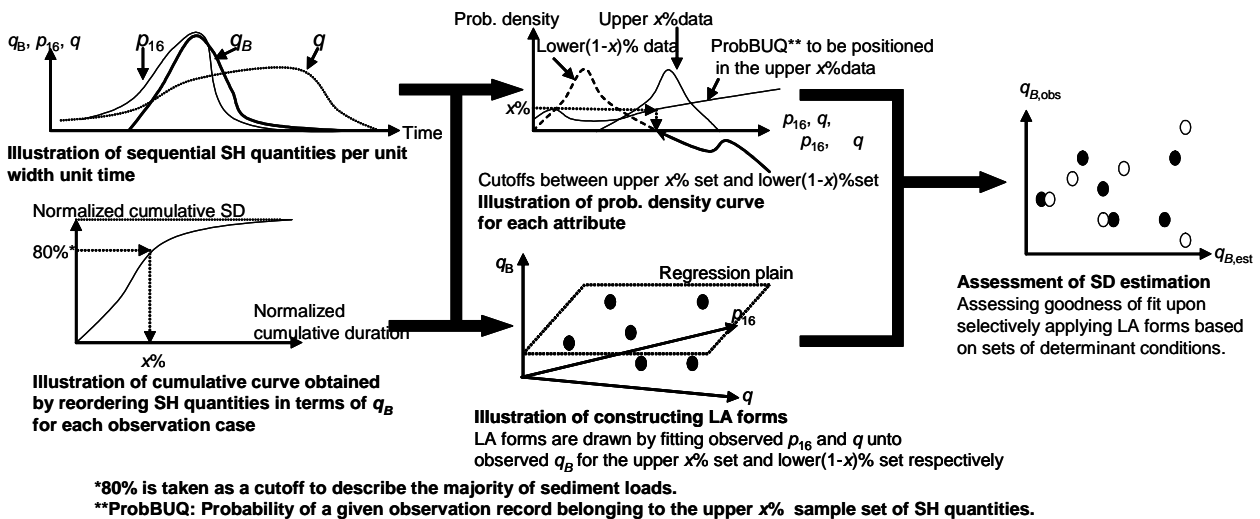


Fig.9 Illustrative view of analytical procedures for each step

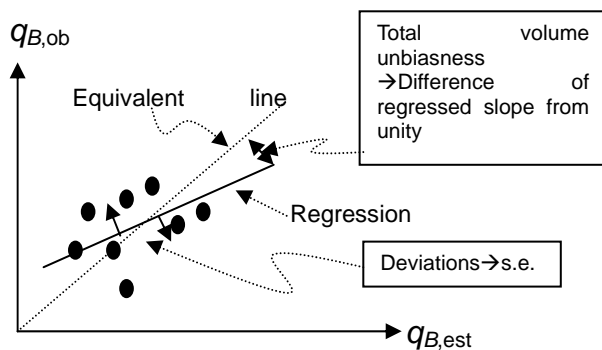


Fig.10 Conceptual view of sequential consistency between estimated and observed sediment discharge

Goodness of fit values for the estimators were tested using VUB and SC as scales. SC was examined using (linear) standard errors (s.e.) and by the distances of q_B ratios from unity (hereafter ‘DOR’), which are defined in Equation (3). Figures 8, 9, and 10 provide an outline of the analytical methods, an illustrative view of the analytical procedures for each step, and a conceptual view of SC between measured and estimated SDs, respectively.

$$DOR \equiv \left| \frac{\sum q_{B,est}}{\sum q_{B,obs}} - 1 \right| \quad (3)$$

Here, $\sum q_{B,obs}$ is a summation of observed q_B and $\sum q_{B,est}$ is a summation of estimated q_B .

4. VARIATION IN CHARACTERISTICS OF SEDIMENT DISCHARGES

Sequential SDs were reordered in a descending pattern, and from them, the time duration that contributed 80% of total sediment loads was obtained for each observation case. This fraction of 80% was considered to represent most of the examined sediment load. Ratios of the time duration of 80% sediment load to the whole flood duration were drawn for all cases. Figure 11 presents the relationships with flood durations and includes the relationships with 50% sediment loads for comparison.

The ratios of the time duration of 80% sediment load to flood duration averaged 2.39×10^{-1} , with a standard deviation of 1.27×10^{-1} , a CV of 5.30×10^{-1} , a lower quartile of 1.54×10^{-1} , and an upper quartile of 2.95×10^{-1} , demonstrating relatively high statistical stability. The reordered set of SH

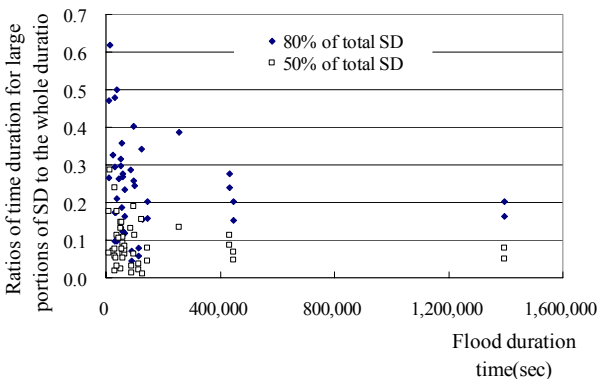


Fig.11 Relationship between flood duration and time ratio needed for a major part of sediment to be discharged for each case

attempt to differentiate concentrated and minor occurrence times solely using indirect methods. The basic SH observation data were dissected into two aggregated sets of concentrated and minor occurrence time, from which corresponding LA forms for q_B , together with SF analytical forms, were derived with independent variables of p_{16} and q . The set of analytical forms was selectively applied to determinant conditions for the entire observation dataset upon on a trial basis.

observation data, summed beginning with the larger values, provided a cumulative (summation) curve of sediment loads and flood durations, normalized by total sediment load and whole flood duration for each case. Figure 12 presents the average normalized cumulative curve.

Most SDs occur within limited periods, in addition to having strong discontinuity, revealing the extremely discrete and concentrated nature of SDs. When SDs were integrated across flood duration, an average of 80% occurred within a 2.39×10^{-1} fraction of flood duration, which is approximately equal to the upper one-fourth of each reordered observation series. In other words, the upper quarter in terms of SD values contributes about 80% of the total sediment load in each case. The set of SH observation data is hereafter dissected into the aggregated upper quarter and the lower three-quarter samples, where the former is the concentrated occurrence time and the latter is the minor occurrence time. SDs, pulses, and FDs were examined, together with their first-order differences from the previous time-step in their time series.

Figure 13 shows the normalized frequency distributions of q_B for the upper-quarter and the lower-three-quarters samples. Table 3 summarizes the averages, standard deviations, and CVs for each quantity and each set of samples.

Analysis of these statistics between the upper quarter and the lower three-quarters revealed that on average, SDs were about 13 times greater in the former (7.06×10^{-5} (m³/sec/m)) than in the latter (5.44×10^{-6} (m³/sec/m)), and the ratios were about 1.19 for average FDs, about 2.59 for average pulses, about 1.24 for flow discharge differences, and about 2.50 for pulse differences. SDs at concentrated occurrence times tended to grow by one order of magnitude beyond those at minor occurrence times, even after eliminating extreme values by the averaging processes; these results far surpass those for FDs, pulses, FD differences, and pulse differences. Differences in the averages between the two sets were all statistically significant, at the 1% level. The probability of a given observation record belonging to the upper-quarter sample set of SH quantities is expressed in Equation (4) according to the definition of probability (hereafter ‘ProbBUQ’).

$$Pr ob(x \in \Omega_{q_B, upper-quarter}) = \frac{Num(x \in \Omega_{q_B, upper-quarter})}{Num(x \in \Omega_{all-q_B})} \quad (4)$$

Here, Prob(x) is a probability density function; Num(x) is a function counting the number of samples in a corresponding set, x represents a given SH variable, and Ω represents the sample set specified by each subscript where $\Omega_{q_B, upper-quarter}$

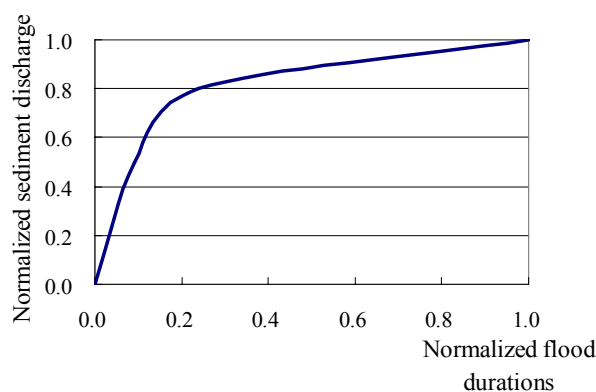


Fig.12 Averaged cumulative curve between flood duration rate and sediment discharge rate for SH data reordered in a descending manner

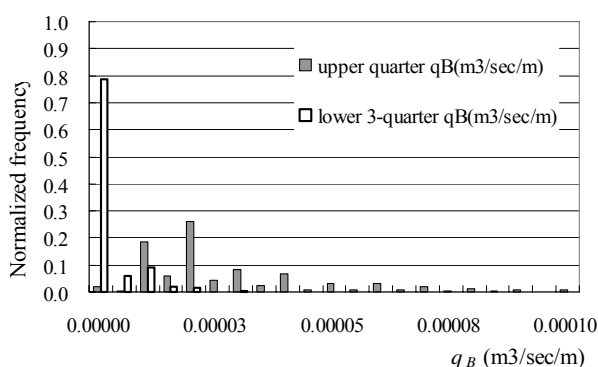


Fig.13 Frequency distribution of unit width sediment discharge for upper quarter samples and lower three-quarter samples

Table 3 Statistics of sediment-hydraulic properties of upper quarter and lower 3-quarters samples

Observation item	Statistics	Upper quarter samples	Lower 3-quarter samples
Sediment discharge	Average	7.06×10^{-5}	5.44×10^{-6}
	Standard Dev.	2.12×10^{-4}	2.79×10^{-5}
	CV	3.01	5.12
Flow discharge	Average	1.05	8.81×10^{-1}
	Standard Dev.	1.09	5.43×10^{-1}
	CV	1.03	6.16×10^{-1}
Pulse	Average	1.26	4.87×10^{-1}
	Standard Dev.	2.06	1.17
	CV	1.63	2.41
Difference of FDs	Average	3.31×10^{-4}	2.66×10^{-4}
	Standard Dev.	4.61×10^{-3}	9.72×10^{-4}
	CV	1.39×10^0	3.66
Difference of pulses	Average	3.02×10^{-4}	1.21×10^{-4}
	Standard Dev.	2.13×10^{-3}	1.18×10^{-3}
	CV	7.07	9.73
Data count		2990	9002

indicates the upper quarter sample set and Ω_{all-qB} indicates the universal set of all observed items.

Figure 14 shows the normalized frequency distributions of p_{16} for the upper-quarter and the lower-three-quarters sets, together with the density curve for ProbBUQ; ProbBUQ grew as pulses

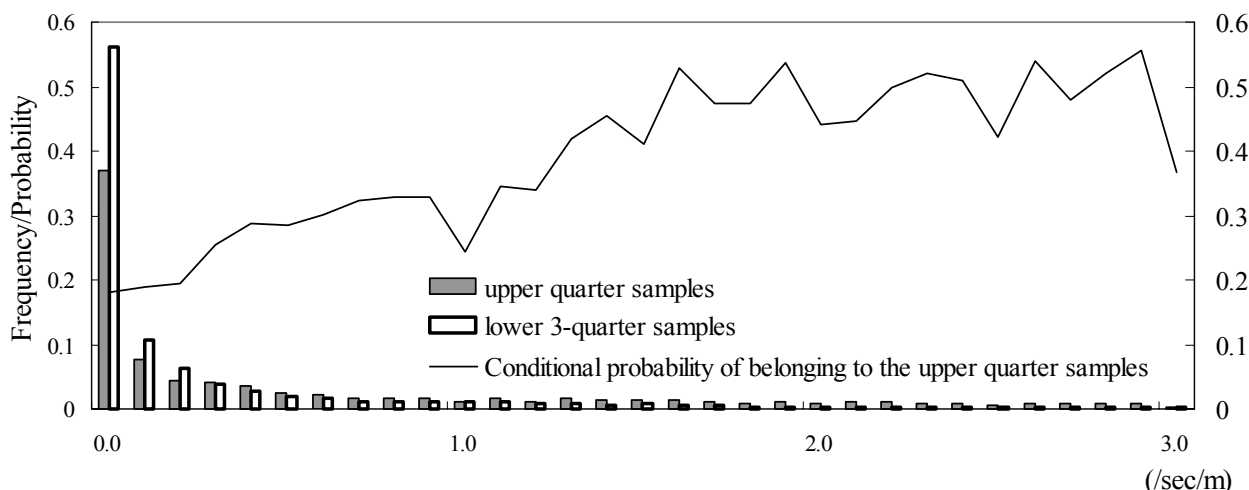


Fig.14 Frequency distribution of unit-width p16 count for upper quarter samples and lower three-quarter samples and of conditional probability of constituting the upper quarter samples

Table 4 Lower limit corresponding to probability 1/4 for each sediment-hydraulic quantities

Cutoffs for the probability of 1/4 (Lower limit)	
Flow discharge	9.0×10^{-1}
Pulses	3.0×10^{-1}
Difference of FD	1.0×10^{-4}
Difference of Pulses	3.0×10^{-4}
	(Upper limit of the lower region, -4.0×10^{-4})

*all in the unit of per one meter and per second

became larger. The default inference probability of assigning a given observation record to the upper quarter is one-fourth, as obtained from the ratio of sample numbers. The inference can be improved by utilizing pulse observation even without SD observation when ProbBUQ exceeds one-fourth in Fig.13. In fact, a good inference can be made blindly using the one-fourth default value whenever ProbBUQ is lower than one-fourth. This finding can be applied to other SH quantities by using similar reasoning. Several possible alternatives are available for determinant conditions to distinguish between the upper-quarter and the lower-three-quarters sets, from which we applied values corresponding to a probability of one in four as the cutoff points.

Table 4 presents values for FD, pulse, FD difference, and pulse difference, which correspond to the probability of one-fourth for all observation cases. Comparative upper quartile values of FDs and pulses without regard to SD q_B were $q = 1.15$ and $p_{16} = 5.54 \times 10^{-1}$, respectively; these values were slightly higher compared to the figure for a probability of one in four. Differences between FDs and pulses were not comparable by the lower limits alone, because the distribution forms themselves exhibited considerable discrepancy. The probability of correctly identifying a given observation record

between the two sets when no information was available was one in four. Whether or not recorded observation items exceeded the values in Table 4 provide a clue to allow better inference.

5. SEDIMENT DISCHARGE ANALYSIS AND EVALUATION

LA forms with pulses and FDs can be constructed as Equations (5) and (6) for the upper-quarter and the lower-three-quarters samples:

$$q_B = 2.82 \times 10^{-5} p_{16} + 9.81 \times 10^{-6} q \quad (5)$$

(VUB: 6.17×10^{-1} , s.e.: 6.23×10^{-5} , DOR: 8.77×10^{-1})

$$q_B = 2.84 \times 10^{-6} p_{16} + 2.36 \times 10^{-6} q \quad (6)$$

(VUB: 7.08×10^{-1} , s.e.: 4.09×10^{-6} , DOR: 8.80×10^{-1}),

where the three values in parentheses refer to VUB, standard errors, and DOR, respectively (the latter two values express SC in their combination) for sample sets of concentrated and minor occurrence times used for coefficient fitting.

Comparison of the coefficients in Equations (5) and (6) revealed that the coefficient for p_{16} was lowered by about one-tenth from the upper-quarter to the lower-three-quarters samples, and that for q was lowered by about one-fourth. The dimension of the coefficient for p_{16} corresponds to sediment volume per pulse, whereas that of q corresponds to sediment density. Sediment-hydraulic interpretation of these coefficients, however, will require further research, as p_{16} -terms and q -terms have unsolved interactions. Individual analytical forms with their coefficients need to be developed to improve the accuracy of SD estimation, as the phenomena differed markedly in concentrated and minor

Table 5 Coefficients and goodness of fit (biases and consistency) of sediment discharge estimated by each analytical form and time unit of analysis

Time unit of analysis	Type of samples	2-factor linear additive analytical forms				Single factor analytical forms			
		p_{16} coefficient (m ³)	q coefficient (m ³ /m ³)	Total volume unbiasedness (VUB)	Sequential consistencies* s.e., DOR	p_{16} coefficient (m ³)	q coefficient (m ³ /m ³)	Sequential consistencies* s(p ₁₆)* s.e., DOR	Sequential consistencies* s(q)* s.e., DOR
Sequential analysis for each observed time	Total observation sample	1.80×10^{-5}	2.86×10^{-6}	6.93×10^{-1}	2.71×10^{-5} 9.20×10^{-1}	3.16×10^{-5}	2.34×10^{-5}	4.57×10^{-5} 8.70×10^{-1}	1.80×10^{-5} 9.55×10^{-1}
	Upper quarter samples	2.82×10^{-5}	9.81×10^{-6}	6.51×10^{-1}	6.23×10^{-5} 8.77×10^{-1}	3.22×10^{-5}	6.71×10^{-5}	1.12×10^{-4} 7.90×10^{-1}	7.29×10^{-5} 8.80×10^{-1}
	Lower 3-quarter samples	2.84×10^{-6}	2.36×10^{-6}	6.36×10^{-1}	4.09×10^{-6} 8.80×10^{-1}	1.12×10^{-5}	6.18×10^{-6}	1.17 9.12×10^{-1}	5.43×10^{-1} 8.80×10^{-1}
Aggregated analysis for each flood case	Total observation sample	3.28×10^{-6}	7.42×10^{-6}	4.18×10^{-1}	9.71×10^{-3} 5.90×10^{-1}	3.18×10^{-5}	2.36×10^{-5}	9.71×10^{-3} 5.82×10^{-1}	1.04×10^{-2} 1.54×10^{-2}

*Standard errors and differences of their ratio from unity, between observed and estimate q_B

occurrence times.

To examine analytical forms, Table 5 summarizes coefficients and goodness of fit for two-factor LA forms and SF forms, all without intercepts. Fitting results for SH quantities aggregated over each flood case, where each flood is represented by one datum, were also tabulated for reference in addition to the sequential fitting results discussed thus far. Fitting with quantities aggregated over each flood case produced statistical consistency across flood cases; this consistency was greater than for SC, as the summation and averaging operations eliminated extreme values. Figure 15 shows SCs by pairs of standard errors and DORs.

SF forms, based on simple proportional relationships, performed better in terms of VUB than did LA forms. For SCs, however, SF forms were inferior to LA forms with regard to standard errors for p_{16} -factor and DOR for q-factor. This finding supports previous reports, which suggested that sequential consistencies of SF forms do not go beyond those of LA forms (Nakaya, 2008a). DORs of two-factor LA forms were greater than were those of p_{16} -SF forms for the upper-quarter samples of concentrated occurrence time, resulting in inferior performance. With regard to standard errors, however, LA forms yielded minimal values, performing better than p_{16} -SF forms. In both indicators of consistencies, LA forms delivered the highest SCs for the lower-three-quarters samples of minor occurrence time, which occupied a large portion of observation duration.

LA forms had a substantial level of SCs with SD phenomena. Furthermore, because the forms expressed in Equations (5) and (6) were calibrated individually to concentrated and minor occurrence times, it was possible to fit them to the phenomena more intricately. Determinant conditions of cutoffs between the upper quarter and the lower three-quarters shown in Table 4 were applied to the

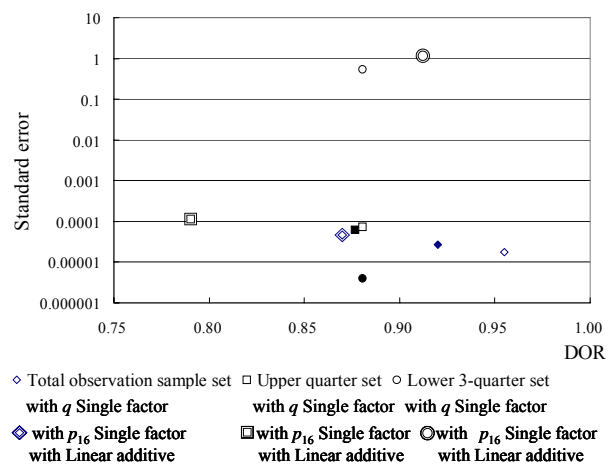


Fig.15 Relationship between two indicators of sequential consistencies for each observation sample

aggregated SH quantities. Equations (5) and (6) were then selectively applied to determine to what degree VUB values were improved. Figure 16 depicts VUBs and SCs of sediment estimators obtained by selectively applying Equations (5) and (6); concentrated and minor occurrence times were distinguished based on the determinant cutoffs corresponding to the probability of one-fourth for FD, pulse, FD difference, and pulse difference individually and in combination. Cases of FD and pulse differences are shown for statistical comparison because their physical implication is yet to be analyzed. Note that the VUBs and SCs in the bottom two lines of Fig. 16, calculated without regard to q_B , are shown only for reference and for the formality of comparison as they were not taken from the same samples used to construct Equations (5) and (6).

In Fig. 16, VUBs are close to unity when SH samples are differentiated by FD and pulse either as single determinant cutoffs or as joint cutoff (the 'and' condition). Determinant conditions by differences in FD and pulse in joint conditions (both

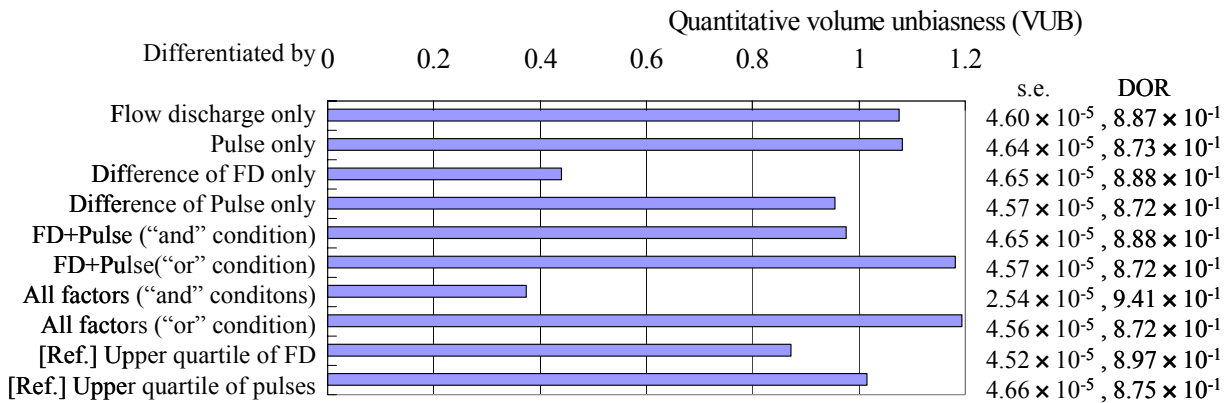


Fig. 16 Quantitative unbiasedness of analytical sediment discharges, differentiating observation sets by cutoffs

'and' and 'or') had little impact in improving VUB. Determinant conditions by differences in pulse only yielded a good statistical property and may help improve estimation upon further physical analysis. SCs with determinant conditions were calculated for the aggregated universal set of SH samples. Both indicators of SCs fell between those for the upper-quarter and those for the lower-three-quarters sets. Application of the determinant condition of FD difference to the aggregated universal set yielded SC values that were as good as those for the lower-three-quarters set, but this worsened VUB values. For reference, the pulse cutoff of the upper quartile improved the VUB most among the determinant conditions obtained without regard to q_B , with similar SCs. This study conducted a bimodal analysis based on direct sampling. As the physical characteristics of pulses continue to be elucidated, it may be possible to develop a way to dissect sets of SH samples by pulses alone.

6. CONCLUSIONS

The discrete and concentrated nature of sediment discharge and transport phenomena has generally been studied qualitatively from a limited number of observation cases. This study conducted a quantitative analysis for 44 minor flood cases at three sites in the Hokuriku region. The results indicate that 80% of sediment discharge during flood durations (when water stages rise and pulses are observed) is concentrated within the aggregated 23.9% (about one-fourth) portion of the duration, and these figures were obtained by reordering and then summing sequences of sediment discharges observed sporadically and discretely. The aggregated and reordered sediment-hydraulic sample set was dissected by the upper quartile in terms of sediment discharge q_B , defining the upper-quarter set as representing the concentrated

occurrence time and the lower-three-quarters set as the minor occurrence time. The upper-quarter set yielded sediment discharges that were, on average, 13 times greater than those of the lower-three-quarters set. Frequency distributions of sediment-hydraulic quantities of the two sets deliver conditional probability density curves from which the probability of a given observation record belonging to the upper-quarter set can be inferred. Conversely, determinant conditions to differentiate the two sets can be obtained by setting the probability of one-fourth and using the probability density curve.

Coefficients of sediment discharge analytical forms were drawn by fitting the forms for the entire sediment-hydraulic observation dataset, the upper-quarter set, and the lower-three-quarters set and the quantitative unbiasedness and sequential consistencies were also assessed in the process. Sequential consistencies, which represent how estimators follow observed phenomena, can be measured by two indicators of standard errors (s.e.) and distances of the q_B estimation/observation ratio from unity. Two-factor linear analytical forms produce better sequential consistency in terms of the two indicators compared with both p_{16} and q single-factor forms.

By applying determinant conditions that differentiate sediment-hydraulic samples by flow discharge and pulse either as single determinant cutoffs or as the joint cutoff (the 'or' condition), we can obtain quantitative unbiasedness close to unity, improving sediment discharge estimation by LA forms.

Our results demonstrated that the quantitative accuracy of sediment discharge analysis, at the time scale of flood events, can be improved by dissecting sediment discharge phenomena into concentrated and minor occurrence times, incorporating variation in sediment discharge during flood durations.

Further observations should ensure a more in-depth physical understanding of the coefficients of sediment discharge of the analytical forms and the differences between those of concentrated and minor occurrence periods. Sediment discharge and transport phenomena will be clarified through consideration of more basic sediment–hydraulic factors, such as the determinant conditions and cutoffs for sediment–hydraulic quantities at concentrated and minor occurrence times, in relation to more static sediment–hydraulic factors at each observation site.

ACKNOWLEDGEMENTS: I am grateful to the staff at the Yuzawa Sabo Office and the Kanazawa River and National Road Office of Hokuriku Regional Development Bureau, Ministry of Land, Infrastructure, Transport, and Tourism, Japan for providing necessary observation data about sediment–hydraulic quantities such as sediment discharges and hydrophone pulses. I also thank Professor Takahisa Mizuyama at the Graduate School of Agriculture, Kyoto University, for providing helpful comments about the investigation and analysis of sediment discharge and hydrophone system pulses.

REFERENCES

- American Society of Civil Engineers (1975): Sedimentation Engineering, ASCE Manuals and Reports on Engineering Practice, No.54, p.190–230
- Ancey, C., Davison, A., Böhm, T., Jodeau, M., and Frey, P. (2008): Entrainment and motion of coarse particles in a shallow water stream down a steep slope, *Journal of Fluid Mechanics* Vol.595, pp.83–114
- Ashida, M., Takahashi, T., and Michiue, M. (1983): Sediment-related disasters in rivers and their countermeasures, Morikita Shuppan Press, pp.20, 26–29
- Ashida, M., Takahashi, T., and Mizuyama, T. (1978): Study on bed load equations for mountain streams, *JSECE*, Vol.30, No.4, pp.9–17
- Bunte, K., Abt, S. R., Potyondy, J. P., and Ryan, S. E. (2004): Measurement of coarse gravel and cobble transport using portable bedload traps, *Journal of Hydraulic Engineering*, Vol.130, No.9, pp.879–893
- D’Agostino, V. and Lenzi, M. A. (1999): Bedload transport in the instrumented catchment of the Rio Cordon Part II. Analysis of the Bedload rate, *Catena* 36, pp.191–204
- Georgiev, B.V. (1990): Reliability of bed load measurements in mountain rivers, *Proceedings of two Lausanne Symposia*, August 1990, IAHS Publ no. 193, 1990, pp.263–270
- Gomez, B. and Church, M. (1989): An assessment of bedload sediment transport formulae for gravel-bed rivers, *Water Resources Research*, Vol.25, pp.1161–1186
- Gomez, Basil (1991): Bedload transport, *Earth-Science Reviews*, 31 (1991) pp.89–132
- Habersack, H.M. and Laronne, J. B. (2002): Evaluation and improvement of bed load discharge formulas based on Helley–Smith sampling in an alpine gravel bed river, *Journal of Hydraulic Engineering*, Vol.128, No.9, pp.484–499
- Habersack, H.M., Nachtnebel, H. P., and Laronne, J.B. (2001): The continuous measurement of bedload discharge in a large alpine gravel bed river, *Journal of Hydraulic Research*, Vol. 39, No.2, pp.125–133
- Hoshino, K., Sakai, T., Mizuyama, T., Satofuka, Y., Kosugi, K., Yamashita, S., Sako, Y., and Nonaka, M. (2004): Sediment monitoring system and some results in the Rokko–Sumiyoshi River, *JSECE*, Vol.56, No.6, pp.27–32
- Imaizumi, F., Yamamoto, T., Tsuchiya, S., and Osaka, O. (2005): Characteristics of the bedload and suspended sediment in a small torrent: Evidence from intense field sampling for understanding sediment transport mechanism, *JSECE*, Vol.57, No.6, pp.13–20
- JSCE (1999): Handbook of Hydraulic Formulas (in Japanese), 1999 edition, JSCE, p.713
- Kleinhans, M. G. and van Rijn, L. C. (2002): Stochastic prediction of sediment transport in sand–gravel bed rivers, *Journal of Hydraulic Engineering*, Vol.128, No.4, pp.412–425
- Kuzuha, Y., Tomosugi, K., Kishio, T., and Hayano, M. (2001): Classification of catchments by hydrologic regimes, *JSHWR*, Vol.14, No.2, pp.131–141
- Lenzi M.A., L. Mao, F. C. (2004): Magnitude–frequency analysis of bedload data in an alpine basin, *Water Resources Research*, Vol.40, W07201, doi:10.1029/2003WR002961
- Lopes, Vincente L., Osterkamp, Waite R., and Bravo-Espinosa, Miguel (2007): A method for improving predictions of bed-load discharges to reservoirs, lakes & reservoirs: *Research and Management*, Vol.12, pp.59–72
- Nakaya, H. (2007): Probabilistic flood discharge analysis in small-scale river basins in Hokuriku region, *JSECE*, Vol.60, No.2, pp.25–32
- Nakaya, H. (2008a): Comparative analysis of sediment discharge estimated by indirect methods and yearly reservoir sedimentation in Hokuriku region, *JSECE*, Vol.61, No.3, pp.3–14
- Nakaya, H. (2008b): A case study of influences on the bed load detection rate of hydrophone system exerted by flow discharges, *JSECE*, Vol.61, No.4, pp.12–20
- Nakaya, H. (2009a): Statistical bed load analysis of small-scale floods based on hydrophone observation, *JSECE*, Vol.61, No.5, pp.4–11
- Nakaya, H. (2009b): Case analysis of flood sediment discharge in a stream segment regulated by a series of sabo dams, *JSECE*, Vol.61, No.6, pp.11–18
- Nakaya, H., Tsuruta, K., and Yoshimura, N. (2007): Sediment discharge observation and its analysis by means of a hydrophone in the upper Tedorigawa river basin, *JSECE*, Vol.60, No.3, pp.25–30
- Rickenmann, D. (1991): Hyperconcentrated flow and sediment transport at steep slopes. *Journal of Hydraulic Engineering*, Vol.117, No.11, pp.1419–1439
- Rickenmann, D. (2001): Comparison of bed load transport in torrents and gravel bed streams. *Water Resources Research*, Vol.37, No.12, pp.3295–3305
- Rickenmann, D. and McArdell, B. W. (2007): Continuous measurement of sediment transport in the Erlenbach stream using piezoelectric bedload impact sensors, *Earth Surface Processes and Landforms*, 32, pp.1362–1378
- Rickenmann, D. and McArdell, B. W. (2008): Calibration of piezoelectric bedload impact sensors in the Pitzbach mountain stream, *Geodinamica Acta*, 21/1–2, pp.35–52
- Torizzo, M. and Pitlick, J. (2003): Magnitude–frequency of bed load transport in mountain streams in Colorado, *Journal of Hydrology*, Vol.290, pp.137–151
- Warburton J. (1992): Observations of bed load transport and channel bed changes in a proglacial mountain stream. *Arctic*

and Alpine Research Vol. 24, No. 3, pp.195–203

Yager, E.M., Kirchner, J.W., and Dietrich, W.E. (2007):
Calculating bedload transport in steep, boulder-bed channels,
Water Resources Research. 43, W07418,
doi:10.1029/2006WR005432